Journal of Exploratory Research in Pharmacology **2026** vol. 11(1) | e00039
DOI: 10.14218/JERP.2025.00039

Original Article

Computational Insights into the Interactions of Andrographolide Derivative SRJ09 with Histone Deacetylase for the Management of Beta Thalassemia

Soumya Khare[1*] and Tanushree Chatterjee[2]

[1]*Department of Biotechnology, Kalyan P.G. College, Bhilai, Chhattisgarh, India;* [2]*Department of Biotechnology, Raipur Institute of Technology, Raipur, Chhattisgarh, India*

Received: July 28, 2025 | **Revised:** September 18, 2025 | **Accepted:** December 12, 2025 | **Published online:** January 14, 2026

Abstract

Background and objectives: Thalassemia is a group of anemias that result from inherited defects in the production of the beta chain of hemoglobin. It is stabilized by gamma globin, which combines to form fetal hemoglobin. One therapeutic approach is to target histone deacetylase (HDAC), which plays an important role in controlling beta thalassemia. This study sought to identify a natural inducer for treating this disease.

Methods: Twenty-five *Andrographis paniculata* compounds were screened using Schrödinger Suite 2020 (Maestro 12.3) for ligand preparation, grid generation, glide extra precision docking and molecular mechanics/generalized born surface area scoring. The HDAC2 crystal structure (Protein Data Bank ID: 4LXZ) was prepared by removing crystallographic water molecules and performing restrained minimization. Top-scoring complexes were subjected to 5-ns molecular dynamics simulations in GROMACS 2019 using the optimized potentials for liquid simulations force field, three interaction site point charge solvation, and standard neutralization and equilibration protocols. Absorption, distribution, metabolism, and excretion properties were predicted using QikProp.

Results: Among the twenty five screened compounds, SRJ09 derivative of andrographolide, ranked among the top candidates based on glide extra precision docking and molecular mechanics/generalized born surface area scores and was therefore selected for further analysis. SRJ09 showed favorable binding to the HDAC2 active site, with interactions comparable to the reference inhibitor 20Y. Absorption, distribution, metabolism, and excretion predictions indicated acceptable drug-likeness, and molecular dynamics simulations demonstrated stable SRJ09–HDAC2 complex behavior over 5 ns.

Conclusions: We concluded that beta thalassemia may benefit from the use of andrographolide, and SRJ 09 as prospective HDAC2 inhibitor drugs that are favourable and efficacious and that generate fetal hemoglobin. Therefore, this bioactive compound is worth further investigation using *in vitro* and *in vivo* studies.

Introduction

Beta thalassemia is a group of hereditary blood disorders characterized by abnormalities in the synthesis of the beta globin chain of hemoglobin. Mutation-caused genetic diseases in the beta globin gene are widely known as human beta-hemoglobinopathies, in which beta thalassemia is most prevalent, particularly in Asia, Africa, and the Mediterranean region.[1] Clinical manifestations include hematopoietic stem cell transplantation, or fetal hemoglobin (HbF) reactivation as an alternative process to cure beta thalassemia.

Several investigations have suggested that chemotherapeutic agents are not suitable for treating β-hemoglobinopathies, such as beta thalassemia, due to their cytotoxicity and growth-inhibitory effects, even when they are effective at inducing HbF production. Based on an examination of the processes behind the HbF inducing drugs effects, a lot of work has gone into discovering novel HbF inducing natural compounds that combine safety, efficacy,

Keywords: Beta thalassemia; Fetal hemoglobin; Histone deacetylase; Bioactive compound; Molecular docking; Molecular dynamics simulation.

***Correspondence to:** Soumya Khare, Department of Biotechnology, Kalyan P.G. College, Bhilai, Chhattisgarh 490006, India. ORCID: https://orcid.org/0000-0003-0477-0996. Tel: +91-7000868305, E-mail: soumyashrivastava82@gmail.com

How to cite this article: Khare S, Chatterjee T. Computational Insights into the Interactions of Andrographolide Derivative SRJ09 with Histone Deacetylase for the Management of Beta Thalassemia. *J Explor Res Pharmacol* 2026;11(1):e00039. doi: 10.14218/JERP.2025.00039.

and convenience of administration to overcome this therapeutic obstacle.

The β globin gene is the sole cause of the alpha-beta globin chain imbalance that leads to severe anemia in patients with beta thalassemia. By stimulating the formation of the γ globin chain, which is primarily expressed in fetuses, this condition can be improved, and adults will produce HbF ($\alpha_2\gamma_2$). Since the transcription of the γ globin gene is gradually inhibited as development advances, low HbF is typically present in normal adults. Nonetheless, a number of pharmaceutical substances have been documented to either promote HbF or suppress the transcription of the γ globin gene. Many pharmacological compounds that reactivate γ globin gene transcription have been identified, such as cytotoxic agents, DNA methyltransferase inhibitors, and histone deacetylase (HDAC) inhibitors. HDAC inhibitors have also been shown to be potent human HbF inducers for treating beta thalassemia.[2]

HbF interferes with polymerized globin chains, whose interactions with each other result in rigidity of cells. Hydroxyurea, 5-azacytidine, decitabine, and cytarabine are the chemotherapeutic agents used for beta thalassemia.[3] Hydroxyurea is a ribonucleotide reductase inhibitor with the ability to inhibit DNA synthesis, whereas 5-azacytidine, decitabine, and butyrate act as DNA methyltransferase inhibitors.[4,5] Because it can prevent DNA synthesis, Hydroxyurea is sometimes referred to as a ribonucleotide reductase inhibitor.[6] Structurally, classes of HDAC2 inhibitors bind the target HDAC to block histone deacetylase and produce an open chromatin conformation, enabling gene activation.[7] Transcription in the γ globin gene promoter is stimulated through histone deacetylase inhibition; HDAC inhibitors or short-chain fatty acids induce transcription from the γ globin gene promoter and, in some patients, can increase the efficiency of γ globin mRNA translation.[8] These effects do not require HDAC activity, but HDAC inhibitors are often potent γ globin inducers. However, short chain fatty acids that inhibit HDACs also inhibit cell proliferation, which is a limiting factor in thalassemia.[9] Hydroxyurea is an FDA approved treatment for sickle cell disease and is also recommended for non-transfusion dependent βthalassemia, although its effectiveness varies among patients and concerns remain regarding adverse effects such as bone marrow suppression.[10] Hence, it is necessary to develop effective inhibitors for beta thalassemia from natural inducers that do not have adverse effects. Natural remedies for treating beta thalassemia by stimulating HbF inducing activities using medicinal plants have been studied for their authenticity, safety, and efficacy.

Computational drug design, including molecular docking and molecular dynamics (MD) simulations, enables rapid screening of bioactive compounds against disease-relevant protein targets. In beta-thalassemia, key targets include mutant hemoglobin subunit beta proteins, which destabilize hemoglobin, and short chain fatty acids as epigenetic modulators, like HDAC2 which regulate erythropoietin. This study aimed to evaluate the binding affinity and stability of *Andrographis paniculata* bioactive compounds against these targets using *in silico* approaches, providing a foundation for developing novel therapeutics.

Much effort has been made to identify naturally occurring inducers and drug treatments that can the synthesis of HbF and promote the expression of the fetal γ globin gene. Natural inducers like *Andrographis paniculata* and their bioactive compounds are known to have efficient biological activities against various diseases, such as anti-microbial, anti-fungal, anti-oxidant, anti-inflammatory, anti-viral, anti-diabetic, anti-cancer, and anti-diarrheal effects.[11]

Medicinal plant-derived bioactive compounds, such as saponins, tannins, flavonoids, phenols, amino acids and proteins, fats and oils, carbohydrates, alkaloids, glycosides, and other phytochemicals, show promising activities when consumed. They play a very important role in the defense mechanism against various disorders and highly pathogenic diseases.[12] The various bioactive compounds have been found to be beneficial for numerous therapeutic uses with fewer adverse effects. To evaluate the efficacy of HbF induction and the underlying molecular pathways, further investigation is needed. By integrating these discoveries and connecting the recognized molecular routes, we have developed a comprehensive model of pharmacological agents induction of HbF. Therefore, this study aimed to evaluate bioactive compounds from *Andrographis paniculata* as potential HbF inducers by assessing their binding affinity and stability with the HDAC2 target using molecular docking, MD simulation, and absorption, distribution, metabolism, and excretion analysis.

Materials and methods

Modelling platform

The computational analysis was performed using Schrödinger Suite 2020, including Maestro v12.3, LigPrep v3.8, Glide Extra Precision (XP) v8.6, Grid Generation, QikProp v6.3, and Prime/molecular mechanics/generalized Born surface area (MM-GBSA) v4.1. MD simulations were conducted using GROMACS 2019, and ADME properties were predicted with the QikProp module.

Biological data

In this study, 25 bioactive molecules were retrieved from PubChem and ChemSketch. The crystal structure of the HDAC2 target was obtained from the Protein Data Bank (PDB),withthe alpha-numeric identity PDB: 4LXZ.

Preparation of the protein

The protein was prepared using Maestro version 12.3. During the process, the missing side and backbone chains were included. The tool provides two options, namely, the preparation wizard and refinement. The X-ray crystallography structure of the target protein (PDB ID: 4LXZ) with a resolution of 1.85 Å was selected for the study. Water molecules occupying the protein structure were not suitable for the docking study and were therefore removed. Finally, the optimization and minimization processes were completed.[13]

Ligand preparation

The twenty five bioactive compounds were prepared as ligand molecules using LigPrep, which generated multiple structures from each input structure with various ionization states, tautomers, stereo chemical characteristics, and ring conformations. Molecules were eliminated based on criteria such as molecular weight or specified numbers and types of functional groups, while maintaining correct chirality for each successfully processed input structure. The OPLS3e force field was used for optimization, producing thelowenergy isomer of each ligand.[14] Finally, ligand molecules were incorporated into the complex structure for docking.

Molecular docking

To test the docking parameters, the twenty five bioactive compounds were docked into the binding site of HDAC2 using the grid based glide ligand docking program in Schrödinger Suite.[15] In this study, Maestro v12.3 was used to perform rigid and flexible

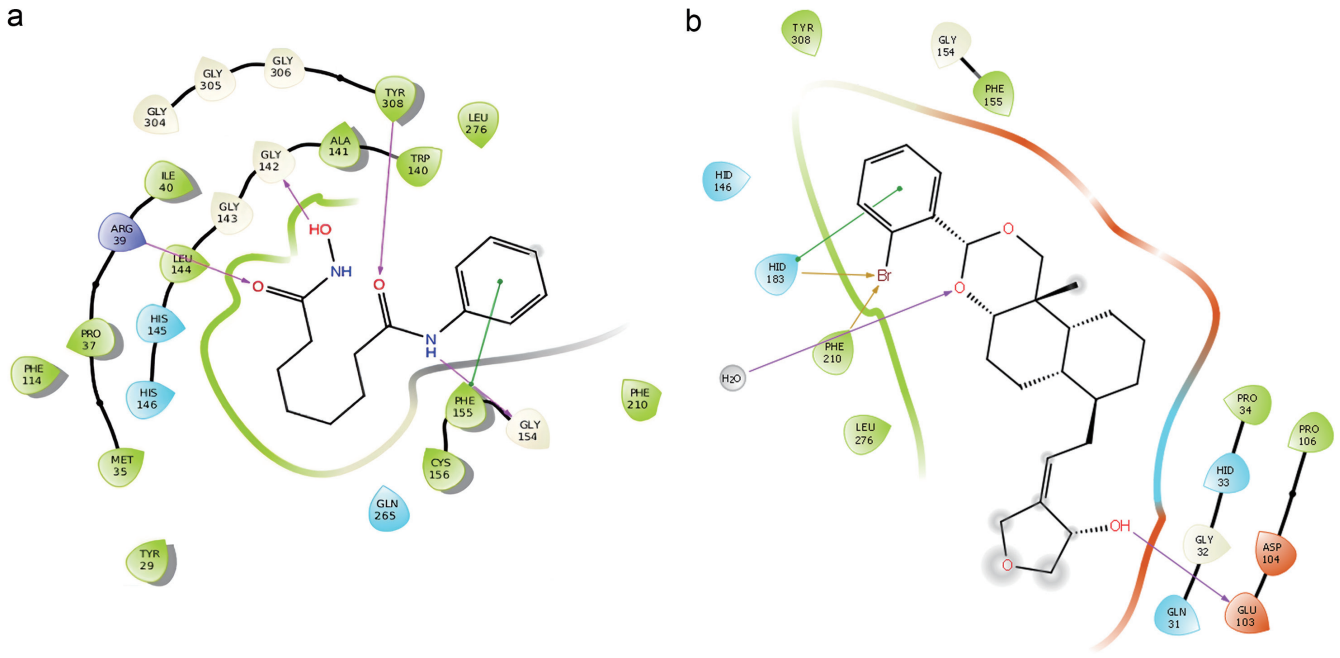

Fig. 1. 2D interaction map of important amino acids with glide extra precision docking target protein (PDB ID: 4LXZ) with (a) 20Y and (b) SRJ09 bioactive compound; residues forming hydrogen bonds are shown in purple. ALA, alanine; ASP, aspartic acid; CYS, cysteine; GLN, glutamine; GLU, glutamic acid; GLY, glycine; HIS, histidine; ILE, isoleucine; LEU, leucine; MET, methionine; PDB, Protein Data Bank; PHE, phenylalanine; PRO, proline; TRP, tryptophan; TYR, tyrosine.

docking to predict binding affinity, ligand efficiency, and inhibitory constant for the target. The ligands were docked to the active site of HDAC2 using glide XP, which considers ligand flexibility. The active small molecule had available access to avoid penalties and received favorable docking scores with accurate hydrophobic contacts between the protein and ligand.[16]

Prime MM-GBSA calculations

The ligand binding energy of each of the twenty five bioactive compounds required to inhibit HDAC2 was estimated using the Prime MM-GBSA module in Schrödinger Suite 2020.[17] This score was then used to rank the ligand-protein glide XP docked complexes.

MD simulation

MD simulations were performed using GROMACS-2019 for 5 ns. The OPLS force field was used for energy calculations to determine protein–HDAC interactions with the ligands. The TIP3P water model was selected to solvate the complexes followed by addition of ions to neutralize the system. The system was solvated in an orthorhombic water box with a 10 Å marginal radius. The protein–ligand complex results were then analyzed. At physiology pH 7.4, the structures were negatively charged; therefore, 10 sodium ions (Na^+) were added to neutralize the system using the GROMACS "genion" tool.[18] Initially, the solvent molecules were relaxed while all solute atoms were harmonically restrained to their original positions with a force constant of 100 kcal/mol for 500,000 steps. Subsequently, the whole system underwent energy minimization for 5,000 iterations using a descent algorithm implementing the OPLS force field.[19] The temperature was maintained at 300 K, and a 2 fs value was used for the integration steps. MD simulations of the protein-ligand complex were performed with position restraints for 500 ps to allow solvent molecules to enter the cavity region of the structure.[20] Finally, MD simulations were performed for 5 ns, and root mean square deviation (RMSD) was calculated to monitor the stability of HDAC2 proteins in their native motion.

ADME toxicity

ADME toxicity analysis is important in drug discovery, especially in determining the mechanism of action of molecules.[21] A set of ADME-related properties was calculated for each of the 25 bioactive compounds using the QikProp program in normal mode. QikProp generates physically relevant descriptors, and the toxicity of a ligand was considered important for its potential as an effective drug in new drug development.[22]

Statistical analysis

Three independent runs of each statistical analysis were conducted using Prism GraphPad Software, and the results were evaluated as mean ± standard deviation. One-way analysis of variance was conducted to ascertain the average differences between antioxidant activity and bioactive compound levels, with p-values < 0.05 considered significant.[23]

Results

Molecular docking HDAC2 (PDB ID: 4LXZ)

Unlike 20Y, the inhibitor bonded to the protein using both glide energy and hydrogen bonds. Hydrogen bond interactions between amino acids and GLU-103 were demonstrated by the amino acids engaging with 20Y (Fig. 1a). In comparison to the protein-bound inhibitor 20Y, which had a glide score of −9.90 kcal/mol, a glide energy of −30.91 kcal/mol, and a glide emodel of −66.43 kcal/mol,

Table 1. Extra Precision Glide Score results of 25 bioactive compounds (ligands) and the energy generated by the active site of the target protein (PDB ID: 4LXZ)

S. no	Bioactive compounds	Docking score (kcal/mol)	XP GScore (kcal/mol)	Glide energy (kcal/Mol)	Glide emodel (kcal/Mol)
Ref	20Y	−9.90	−9.90	−30.91	−66.43
1	SRJ09	−6.83	−6.83	−27.40	−33.66
2	6,10-dimethyl-2-undecanone	−6.56	−6.56	−32.59	−35.84
3	3-pentadecylphenol	−5.77	−5.77	−43.76	−39.69
4	14-alpha-lipoylandrographolide	−5.52	−5.52	−33.41	−58.25
5	SRJ 23	−5.11	−5.11	−37.67	−43.06
6	DRF 3188	−4.52	−4.52	−31.51	−47.62
7	5-hydroxy-7,8-dimethoxyflavone	−4.50	−4.50	−31.78	−39.65
8	14-deoxyandrographolide	−4.06	−4.06	−26.65	−32.08
9	DL-alphatocopherol	−3.90	−3.90	−29.01	−32.70
10	Andrographolide	−3.85	−3.85	−26.37	−31.47
11	3,19-O-diacetylanhdroandro	−3.77	−3.77	−34.67	−36.79
12	Andrograpanin	−3.70	−3.70	−26.60	−27.90
13	14-glycinylandrographolide hydrochloride	−3.61	−3.61	−23.53	−42.16
14	Isoandrographolide	−3.53	−3.53	−32.55	−29.34
15	12-hydroxy-14-dehydroandro	−3.48	−3.48	−36.89	−33.38
16	14-acetylandrographolide	−3.32	−3.32	−23.71	−33.53
17	14-deoxy11,12-didehydroandrographolide	−3.29	−3.29	−22.33	−27.20
18	3,19-isopropylideneandrographolide	−3.27	−3.27	−24.16	−32.55
19	14-Deoxy14,15-Didehydroandrographolide	−3.26	−3.26	−29.43	−35.67
20	5-hydroxy-7,8,2′,5′-tetraimethoxyflavano	−3.25	−3.25	−31.39	−28.22
21	19-O-acetylanhdroandrographolide	−3.19	−3.19	−21.16	−34.95
22	5-hydroxy-7,8,2′,3′-tetraimethoxyflavone	−3.25	−3.25	−3.25	−28.22
23	1-isopropyl-4-methylbicyclo[3.1.0]hex-3-en-2-one	−3.16	−3.16	−3.16	−27.85
24	Neoandrographolide	−3.17	−3.17	−3.17	−33.38
25	1-(But-1-En-3-Ynyl)Benzene	−3.07	−3.07	−3.07	−30.58

PDB, Protein Data Bank.

the bioactive compound SRJ09 shared one hydrogen bond interaction with GLU-103 (Fig. 1b), docked with a glide score of −6.83 kcal/mol, glide energy of −27.40 kcal/mol, and glide emodel of −33.66 kcal/mol (Table 1).

In contrast to the parent drug, which showed a non-phase-specific cell cycle arrest, SRJ09 exhibited a particular G1 phase cell cycle arrest in MCF-7 cells.[24] It is noteworthy that SRJ09 was more effective at inducing apoptosis, indicating that biological consequences differ depending on the location of the bromine substituent in the aromatic ring. Phase-specific cell cycle blocking agents and strong apoptosis inducers may be created by adding a benzylidene pharmacophore at the 3,19-positions of the andrographolide structure.[25]

Prime Molecular Mechanics with Generalized Born and Surface Area (MMGBSA) analysis

Ligand-binding orientation by Prime MMGBSA analysis of HDAC2 target protein (PDB ID: 4LXZ) with bioactive compounds was performed using MMGBSA simulations to determine which ligand binding method was most dependable. The most dependable ligand orientation was determined by comparing the best binding Gibbs free energy that was achieved. It is possible to develop a thorough analysis of the ligand-receptor interaction, which can be very helpful in highlighting the most important interactions and aiding in the design of new active ligands. This is because each receptor residue has an interaction with the ligand and allows evaluation of the individual energy terms of the binding Gibbs free energy.[26]

The protein–ligand complex was stabilized as a result of the minute ligand conformational changes brought about by MMGBSA in the protein active site. Because of its great importance, we used the MMGBSA method to investigate the relative binding strengths of 20Y and SRJ09. MMGBSA values of −34.1 kcal/mol and −28.2 kcal/mol, respectively, indicate a stable system

Table 2. MMGBSA binding Gibbs free energy calculations observed in target protein (PDB ID: 4LXZ) with bioactive compounds 20Y and SRJ09

Protein	Bioactive compounds (ligands)	MMGBSA dGbind kcal/ mol
PDBID:4LXZ	20Y	-34.1
	SRJ09	-28.2

MMGBSA, Molecular Mechanics with Generalized Born and Surface Area; PDB, Protein Data Bank.

that releases energy upon binding (Table 2). These values are negative, which suggests that the systems are stable and that binding releases energy. The strength of the interactions between the binding partners is reflected in the magnitude of the binding energy. Higher complex stability and stronger binding are indicated by more negative results. Complementarily, differences in molecular architectures and the type of intermolecular interactions can explain the variations in binding energy among the systems. The ligand glide energy value and the MMGBSA calculations were among the significant results displayed by the computational study at the conclusion of this analysis. Improved agreement between computed binding affinities and experimental data is provided by physics-based approaches.[27] When compared to docking scoring functions, the current study's MMGBSA methodology yielded impressive results. It was able to establish a stronger correlation between the biological activity of a variety of HDAC2 inhibitors and their predicted binding Gibbs free energies.

Physicochemical and drug-likeness analysis by ADME analysis

One key technique for analyzing a drug's molecular efficacy is the ADME based study. In addition to being effective, a medicine should be able to cross a variety of obstacles to trigger the desired effect at the intended site of action. Lately, time-consuming and laborious experimental procedures have been replaced by the availability of *in silico* methods for quickly predicting pharmacokinetic and toxicity properties, such as absorption, distribution, metabolism, and excretion (ADME) of newly discovered compounds in the human body.[28] As a result, this work used the QikProp tool to analyze the important pharmacokinetic features of the top five bioactive compounds of the HDAC2 target protein (PDB ID: 4LXZ) that demonstrated higher docking scores. The bioactive molecular weight, solvent accessible surface area, QPlogPw (solvation free energy in water), central nervous system, donor hydrogen bond, acceptor hydrogen bond, human oral absorption, and Lipinski's rule of five and three were among the physicochemical characteristics analyzed.[29] All of these are listed in (Table 3). Initially, we evaluated the compounds' oral bioavailability by applying Lipinski's rule of five. All compounds demonstrated good oral bioavailability and passed the drug-likeness test. The outcomes demonstrated that SRJ09 met all requirements. The five bioactive compounds were found to be well absorbed in the gut because they all matched the range for human oral absorption and solvent accessible surface area permeability (Table 3). The compounds were also examined for various drug-like qualities. The Lipinski (Pfizer) filters were passed by all compounds. Additionally, the bioactive compounds demonstrated success in the QPlogPw, human oral absorption parameter and central nervous system. Table 3 provides

Table 3. Summary of ADMET analysis, physicochemical properties, and biological functions of the top five bioactive compounds with higher docking scores of target protein 4LXZ analyzed using QikProp

Bioactive compounds (4LXZ)	MW(Da)[a]	CNS[b]	SASA[c]	Donor HB[d]	Accept HB[e]	polrz[f]	logPw[g]	logPo/w[h]	logS[i]
20Y	264.32	−2	584.04	3	6.7	28.60	15.06	0.75	−2.03
SRJ09	477.43	1	696.28	1	6.8	46.06	10.35	4.87	−6.20
6,10-dimethyl-2-undecanone	198.34	0	488.48	0	2	22.73	1.43	3.53	−3.12
3-pentadecylphenol	304.51	−1	747.73	1	0.75	36.94	1.76	6.83	−7.25
14-alpha-lipoylandrographolide	536.78	−2	840.57	1	7.7	52.77	9.33	5.94	−7.25
SRJ23	477.43	1	659.04	1	6.8	44.25	10.0	4.60	−5.519

Bioactive compounds (4LXZ)	logHERG[j]	logBB[k]	PMDCK[l]	logKp[m]	metab[n]	logKhsa[o]	Human oral absorption[p]	Rule of five[q]	Rule of three[r]
20Y	−4.26	−1.69	110.95	−3.02	3	−0.77	3	0	0
SRJ09	−5.10	0.20	5,734.44	−1.22	4	0.71		0	1
6,10-dimethyl-2-undecanone	−3.33	−0.32	1,875.16	−1.64	1	0.21	3	0	0
3-pentadecylphenol	−6.03	−0.96	1,618.56	−0.58	2	1.36	1	1	1
14-alpha-lipoylandrographolide	−4.83	−1.09	1,199.16	−2.59	6	1.07	1	2	1
SRJ23	−4.51	0.24	5,696.65	−1.23	4	0.62	3	0	0

[a]Molar weight (range for 95% of drugs: 130–725 Da); [b]Predicted central nervous system activity on a (–2 inactive) to (+2 active) scale; [c]SASA (total solvent accessible surface area) in (300.01000.0); [d]Number of hydrogen bonds donated by the molecule (range for 95% of drugs: 0–6).; [e]Number of hydrogen bonds accepted by the molecule (range for 95% of drugs: 2–20); [f]Predicted polarizability (13.070.0 for 95% of drugs); [g]Predicted water/gas partition coefficient (4.045.0); [h]Partitioning coefficient between n-octanol and water phases (range for 95% of drugs: −2 to 6.5); [i]Predicted aqueous solubility (–6.5–0.5); [j] Predicted IC50 value for blockage of HERG K+channels (concern< −5); [k]predicted blood/brain barrier partition coefficient (range for 95% of drugs: −3.0 to 1.0); [l]Predicted apparent MDCK cell permeability in nm/sec (<25 poor, >500 great); [m]Predicted skin permeability (−8.0 to −1.0 for 95% of drugs); [n]Number of likely metabolic reactions (range for 95% of drugs: 1–8);Predicted binding constant to human serum albumin (range for 95% of drugs: −1.5 to 1.5); [p]Predicted qualitative human oral absorption: 1, 2, or 3 for low, medium, or high; [q]Number of violations of Lipinski's rule of five, maximum 4; [r]Number of violations of Jorgensen's rule of three maximum 3. ADMET, absorption, distribution, metabolism, excretion, and toxicity; CNS, central nervous system; HB, hydrogen bond; HERG, human ether-a-go-go-related gene; MDCK, Madin-Darby canine kidney; MW, molecular weight; SASA, solvent accessible surface area.

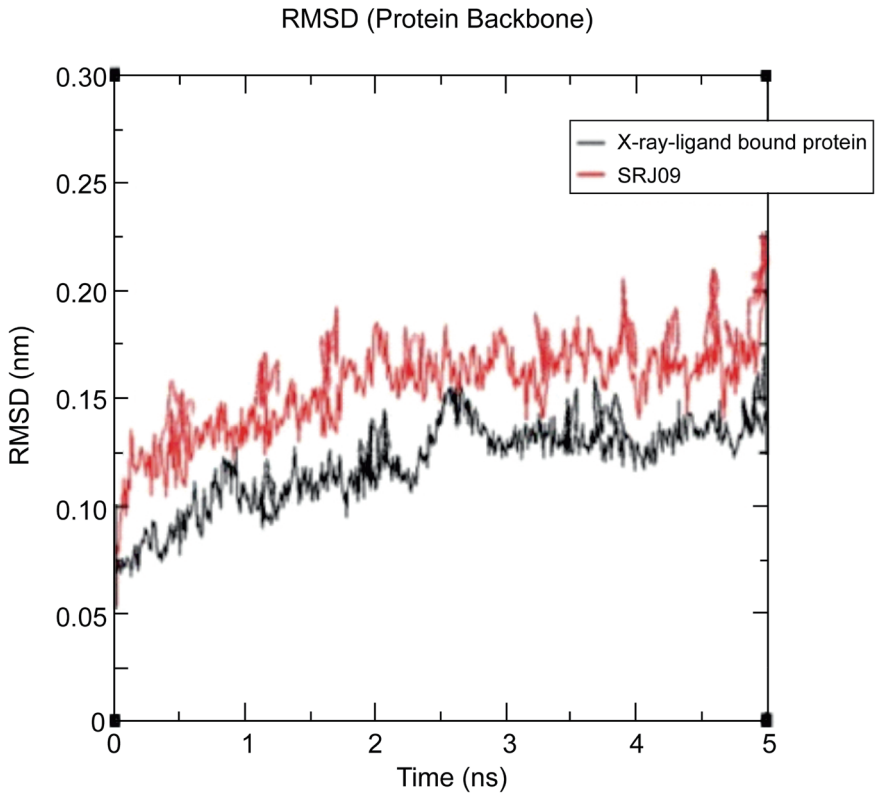

Fig. 2. Plot of RMSD during 5 ns molecular dynamics simulation of target protein (PDB ID: 4LXZ) of HDAC2 in complex with bioactive compounds 20Y and SRJ09. HDAC, histone deacetylase; PDB, Protein Data Bank; RMSD, root mean square deviations.

a summary of the pharmacokinetic property data with a reference parameter range. Furthermore, the bioactive compounds underwent several drug-likeness characteristic screenings. None of these bioactive substances passed the polarizability or skin permeability tests. However, the compounds demonstrated success in the blood-brain barrier parameter.

Molecular dynamic simulation (MDS)

Using MDS made it easier to precisely analyse how biological macromolecules behaved in regulated physiological environments. The flexibility and structural variations of docked complexes could be noticed over the simulation period in a biophysical system. MDS is a computational tool used to analyse the physical interactions in this system.[30] Since determining the essential intermolecular interactions of the bound ligands and their binding stability with the HDAC2 active site was the main goal of this MDS study, three chosen bioactive compounds that displayed higher docking scores were analyzed utilizing molecular docking in the MD simulation for HDAC2. Using GROMACS 2019, the radius of gyration (Rg) values as a function of timeand Root Mean Square Deviation and Fluctuation (RMSD/F) were calculated. The behavior of the projected complex was examined for SRJ09 bound to the target protein (PDB ID: 4LXZ), which was run for 5 ns to account for protein flexibility. By analyzing the trajectories over the 5 ns time function within the solvated medium, we derived important information on the dynamic activity of the tested substances through the use of MDS. The alterations in protein-unbound and protein-bound ligand complexes were examined under physiological conditions using a range of metrics, including gyration radius, intermolecular hydrogen bond formation, RMSDs for each ligand and backbone atom, and root mean square fluctuation (RMSF) for each individual amino acid.

RMSD

By comparing the simulation time to the RMSD of the protein backbone atoms, all of the chosen docked complexes' minor structural and conformational changes were evaluated. Referring to the RMSD from the crystal structure, Figure 2 illustrates how the RMSD values in the target protein (PDB ID: 4LXZ-20Y) complex showed very little fluctuation; it reached stability at 5 ns, at 0.34 nm, and no additional substantial deviation was seen. Throughout the simulation, the RMSD value steadily grew from 0 to 5 ns and achieved a steady level. Figure 2 shows that SRJ09 had average RMSD values of 0.31 nm, respectively.

RMSF

The displacement of a specific atom or set of atoms in relation to the reference structure, averaged over the total number of atoms, is known as the RMSF. This measure works particularly well for examining the flexibility of individual residues inside the protein backbone. The RMSF analysis of the complex PDB ID: 4LXZ-SRJ09 is shown in (Fig. 3). Furthermore, average RMSF values were computed in relation to the 0–5 ns simulation timescale. For the target protein PDB ID: 4LXZ-20Y protein complex, the average RMSF of HDAC2 over 0 to 5 ns simulation was 0.1 nm. The RMSF values indicated that the residues in the β-sheet portions of each complex fluctuated less, even though no significant differences in values were seen in any system. Ideally, andrographolide showed

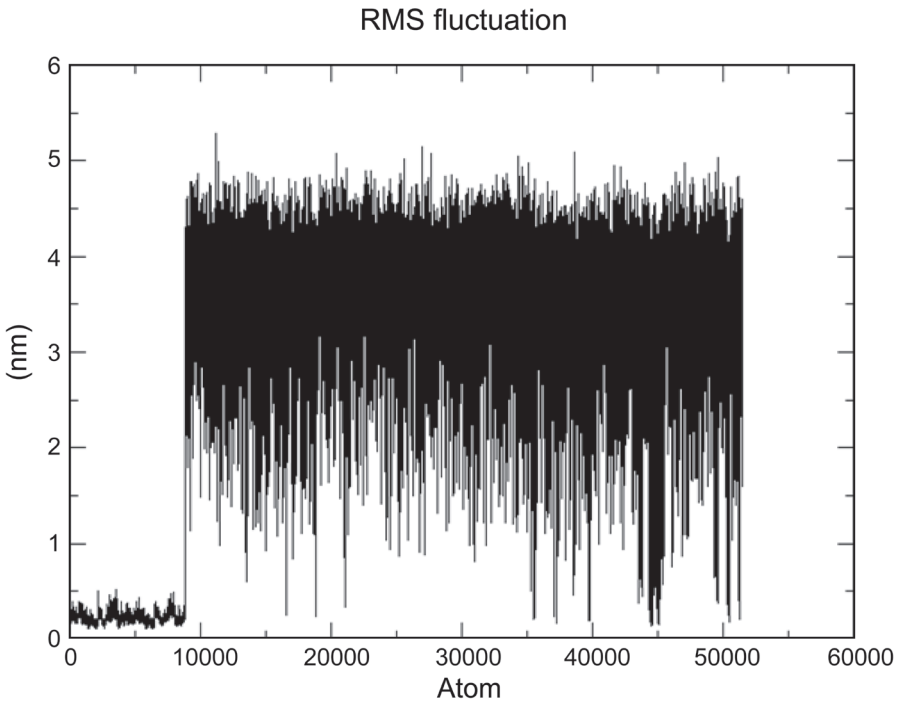

Fig. 3. Plot of RMSF values, during 5 ns molecular dynamics simulation of target protein (PDB ID: 4LXZ) of HDAC2 in complex with bioactive compounds 20Y and SRJ09. HDAC, histone deacetylase; PDB, Protein Data Bank; RMSF, root mean square fluctuation.

larger RMSF fluctuations, while SRJ09 had reduced variation.

Rg

The MDS Rg is an essential parameter for assessing the structural integrity and compactness of a protein, which ultimately determines the stability of the system. The mass-weighted root mean square distance of an atom from its centerof mass is known as the Rg. Figure 4 illustrates the folding competency of the overall structure at various points along the trajectory and shows the time-dependent Rg analysis for the simulated complexes. PDB ID: 4LXZ-SRJ09 complex proteins had average Rg values of 2.4 nm from 0 to 5 ns. The minor variations in the protein Rg values when complexes with PDB ID: 4LXZ-SRJ09 indicates that there was no discernible variation in the complex's folding during the simulation (Fig. 4). This implies that the protein complex maintained its structural stability. The compactness of a structure is measured by its Rg. A stable binding position was indicated by the Rg values of HDAC2 with SRJ09, which remained around 2.4 nm and stabilized between 1 and 5 ns (Fig. 4).

Therefore, the stability of protein-ligand complexes was verified by the MD simulation study of specific docked complexes. The experimental data were confirmed by the low energy values found in our simulations, which raise the prospect that flavones and diterpenoids may interact with HDAC2. Aromatic interactions between TYR-308 and flavones may enhance flavone binding in HDAC2 inhibitors. In the current investigation, we discovered that all three of the putative HDAC2 inhibitors formed a hydrogen bond with the active site residue TYR-308.

Discussion

One of the main aims of computational-based bioinformatics is to find potential drug candidates that will boost the effectiveness, efficiency, and shorten the time required for drug development. Accordingly, we used twenty-five bioactive compounds from *An-*

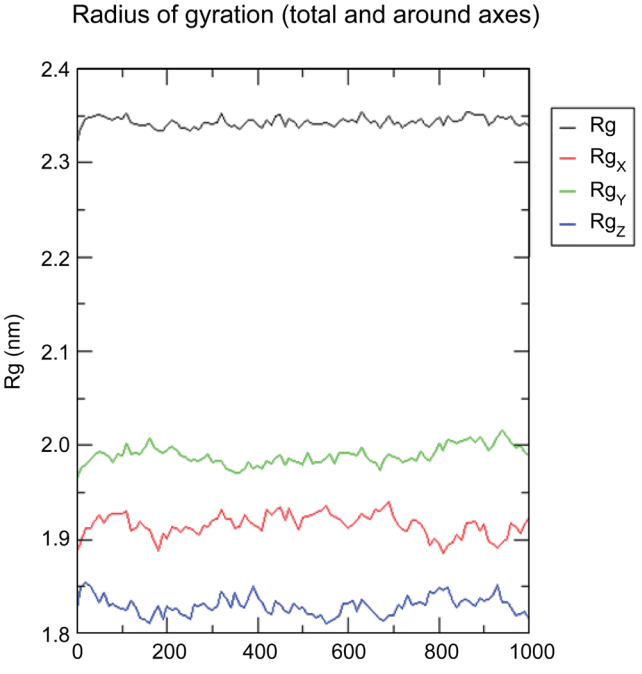

Fig. 4. Plot of radius of gyration (Rg) during 5 ns molecular dynamics simulation of target protein (PDB ID: 4LXZ) of HDAC2 in complex with bioactive compounds 20Y and SRJ09. HDAC, histone deacetylase; PDB, Protein Data Bank.

drographis paniculata as starting compounds in this study and virtually screened structurally similar compounds in the PubChem database, considering the minimal toxicity, good compatibility, and high oral bioavailability that were previously reported. The screened compounds were further reduced using molecular docking, MD simulation, and MMGBSA analysis in order to find possible hit compounds. The PubChem database, which offers a large library of ligands useful for 3D molecular docking, was used in this investigation. Approximately twenty-five bioactive compounds were selected as ligands, and molecular docking was carried out against PDB ID: 4LXZ. The HDAC2 target protein (PDB ID: 4LXZ) has an active binding site with amino acids including GLU103. Furthermore, the ligand SRJ09 was demonstrated to be well bound in the active site of PDB ID: 4LXZ. The MDS study yielded satisfactory RMSD and RMSF findings for the bioactive compounds, including SRJ09, with no discernible instability observed. Over the course of a 5 ns simulation, all complexes remained stable. Furthermore, an area that appeared substantially less flexible in SRJ09 was identified by comparing RMSF versus residue number. Amino acids in these regions interacted differently with SRJ09, indicating that the structural rigidity of the ligand-bound complexes was enhanced by the lower RMSF values.[29] However, significant changes were not seen, and the majority of residues had RMSF values comparable to those of SRJ09, indicating the preservation of well-organized regions both during and after complex formation. We used simulated trajectory-based MM-GBSA outputs to correlate the binding of SRJ09 with the target protein PDB ID: 4LXZ in order to determine the binding energy value for the chosen compounds. It is widely recognized that the stability of ligand-bound complexes is largely dependent on the presence of hydrogen bonds.

According to recent research, the andrographolide derivative SRJ09, and especially its analogues, provide a new avenue for pharmacological research that could advance the treatment of a variety of illnesses, including infections and cancer.[31] A preliminary study was conducted to assess the cytotoxic effect of SRJ09 against the MCF-7 (breast) and HCT-116 (colon) cancer cell lines, evaluating its effects on cell cycle progression and induction of apoptosis.[32] SRJ09 showed a specific G_1 phase cell cycle arrest in MCF-7 cells, unlike the parent compound, which showed a non-phase-specific cell cycle arrest. Notably, SRJ09 induced apoptosis more potently, suggesting that changes in the position of the bromine substituent in the aromatic ring produce different biological outcomes.[33] By adding a benzylidene pharmacophore at the 3,19-positions of the andrographolide structure, it is possible to produce phase-specific cell cycle-blocking agents and potent apoptosis inducers.[34]

Although the computational workflow provided useful preliminary insights, this study is inherently limited by its exclusive reliance on *in-silico* data. The docking and MD results were based on a single HDAC2 crystal structure and may not fully reflect the protein's conformational variability or isoform differences. In addition, ADME properties were predicted using computational models, which cannot substitute for experimental pharmacokinetic or toxicity assessments. Therefore, the therapeutic potential of SRJ09 and related compounds still requires validation through systematic *in-vitro* and *in-vivo* studies.

Conclusions

The plant *Andrographis paniculata* contains anti-bacterial, anti-inflammatory, and antioxidant qualities that strengthen the immune system. The HDAC inhibitors have also been shown to be potent human fetal hemoglobin inducer to treat beta thalassemia. The finding of SRJ09 derivative of andrographolide, a good docking score with binding affinity for the active site of HDAC2. Glide score and glide energy of 20Y (an HDAC2 inhibitor of target protein) showed similar binding affinity to SRJ09 with bioactive compounds of *Andrographis paniculata* plant. The results showed that SRJ09 had complied with all ADME requirements. The MDS study produced acceptable RMSD and RMSF results of the bioactive compounds. There was no observable instability between SRJ09 at 5ns molecular dynamic simulation. We concluded that beta thalassemia may manage by the SRJ09 as prospective HDAC2 inhibitor drugs that efficacious. These in-silico findings suggest that SRJ09 may serve as a promising HDAC2 targeting candidate for inducing HbF and potentially managing beta-thalassemia. However, because this study relied solely on computational data, experimental validation through systematic *in-vitro* and *in-vivo* studies is essential to confirm its therapeutic relevance.

Acknowledgments

None.

Funding

None.

Conflict of interest

The authors declare that there are no conflicts of interest.

Author contributions

Study concept and design (SK, TC), acquisition of data (SK), analysis and interpretation of data (SK), drafting of the manuscript (SK), critical revision of the manuscript for important intellectual content (SK, TC), administrative, technical, or material support (SK), and study supervision (TC).

Ethical statement

Not Applicable.

Data sharing statement

No additional data are available.

References

[1] Ng NY, Ko CH. Natural Remedies for the Treatment of Beta-Thalassemia and Sickle Cell Anemia-Current Status and Perspectives in Fetal Hemoglobin Reactivation. Int Sch Res Notices 2014;2014:123257. doi:10.1155/2014/123257, PMID:27350962.

[2] Mukherjee M, Rahaman M, Ray SK, Shukla PC, Dolai TK, Chakravorty N. Revisiting fetal hemoglobin inducers in beta-hemoglobinopathies: a review of natural products, conventional and combinatorial therapies. Mol Biol Rep 2022;49(3):2359–2373. doi:10.1007/s11033-021-06977-8, PMID:34822068.

[3] El-Beshlawy A, Hamdy M, El Ghamrawy M. Fetal globin induction in beta-thalassemia. Hemoglobin 2009;33(Suppl 1):S197–S203. doi:10.3109/03630260903351882, PMID:20001626.

[4] Bianchi N, Zuccato C, Lampronti I, Borgatti M, Gambari R. Fetal

Hemoglobin Inducers from the Natural World: A Novel Approach for Identification of Drugs for the Treatment of {beta}-Thalassemia and Sickle-Cell Anemia. Evid Based Complement Alternat Med 2009;6(2):141–151. doi:10.1093/ecam/nem139, PMID:18955291.

[5] Fathallah H, Atweh GF. Induction of fetal hemoglobin in the treatment of sickle cell disease. Hematology Am Soc Hematol Educ Program 2006;2006(1):58–62. doi:10.1182/asheducation-2006.1.58, PMID: 17124041.

[6] Perrine SP, Castaneda SA, Boosalis MS, White GL, Jones BM, Bohacek R. Induction of fetal globin in beta-thalassemia: Cellular obstacles and molecular progress. Ann N Y Acad Sci 2005;1054:257–265. doi:10.1196/annals.1345.033, PMID:16339673.

[7] Cao H, Stamatoyannopoulos G, Jung M. Induction of human gamma globin gene expression by histone deacetylase inhibitors. Blood 2004;103(2):701–709. doi:10.1182/blood-2003-02-0478, PMID:12920038.

[8] Pace BS, White GL, Dover GJ, Boosalis MS, Faller DV, Perrine SP. Short-chain fatty acid derivatives induce fetal globin expression and erythropoiesis in vivo. Blood 2002;100(13):4640–4648. doi:10.1182/blood-2002-02-0353, PMID:12393583.

[9] Perrine SP. Fetal globin induction—can it cure beta thalassemia? Hematology Am Soc Hematol Educ Program 2005;2005(1):38–44. doi:10.1182/asheducation-2005.1.38, PMID:16304357.

[10] Yasara N, Premawardhena A, Mettananda S. A comprehensive review of hydroxyurea for β-haemoglobinopathies: the role revisited during COVID-19 pandemic. Orphanet J Rare Dis 2021;16(1):114. doi:10.1186/s13023-021-01757-w, PMID:33648529.

[11] Atanasov AG, Waltenberger B, Pferschy-Wenzig EM, Linder T, Wawrosch C, Uhrin P, *et al*. Discovery and resupply of pharmacologically active plant-derived natural products: A review. Biotechnol Adv 2015;33(8):1582–1614. doi:10.1016/j.biotechadv.2015.08.001, PMID:26281720.

[12] Khanal M, Acharya A, Maharjan R, Gyawali K, Adhikari R, Mulmi DD, *et al*. Identification of potent inhibitors of HDAC2 from herbal products for the treatment of colon cancer: Molecular docking, molecular dynamics simulation, MM/GBSA calculations, DFT studies, and pharmacokinetic analysis. PLoS One 2024;19(7):e0307501. doi:10.1371/journal.pone.0307501, PMID:39037973.

[13] Wang J, Kollman PA, Kuntz ID. Flexible ligand docking: a multistep strategy approach. Proteins 1999;36(1):1–19. PMID:10373002.

[14] Elokely KM, Doerksen RJ. Docking challenge: protein sampling and molecular docking performance. J Chem Inf Model 2013;53(8):1934–1945. doi:10.1021/ci400040d, PMID:23530568.

[15] Binkowski TA, Jiang W, Roux B, Anderson WF, Joachimiak A. Virtual high-throughput ligand screening. Methods Mol Biol 2014;1140:251–261. doi:10.1007/978-1-4939-0354-2_19, PMID:24590723.

[16] Meng XY, Zhang HX, Mezei M, Cui M. Molecular docking: a powerful approach for structure-based drug discovery. Curr Comput Aided Drug Des 2011;7(2):146–157. doi:10.2174/157340911795677602, PMID:21534921.

[17] Hayes JM, Archontis G. MM-GB(PB)SA Calculations of Protein-Ligand Binding Free Energies. Wang L (ed). Molecular Dynamics - Studies of Synthetic and Biological Macromolecules. London: IntechOpen; 2012. doi:10.5772/37107.

[18] Du J, Sun H, Xi L, Li J, Yang Y, Liu H, *et al*. Molecular modeling study of checkpoint kinase 1 inhibitors by multiple docking strategies and prime/MM-GBSA calculation. J Comput Chem 2011;32(13):2800–9. doi:10.1002/jcc.21859, PMID:21717478.

[19] Lee MS, Olson MA. Comparison of volume and surface area nonpolar solvation free energy terms for implicit solvent simulations. J Chem Phys 2013;139(4):044119. doi:10.1063/1.4816641, PMID:23901972.

[20] Hollingsworth SA, Dror RO. Molecular Dynamics Simulation for All. Neuron 2018;99(6):1129–1143. doi:10.1016/j.neuron.2018.08.011, PMID:30236283.

[21] Lin J, Sahakian DC, de Morais SM, Xu JJ, Polzer RJ, Winter SM. The role of absorption, distribution, metabolism, excretion and toxicity in drug discovery. Curr Top Med Chem 2003;3(10):1125–54. doi:10.2174/1568026033452096, PMID:12769713.

[22] Katsila T, Spyroulias GA, Patrinos GP, Matsoukas MT. Computational approaches in target identification and drug discovery. Comput Struct Biotechnol J 2016;14:177–184. doi:10.1016/j.csbj.2016.04.004, PMID:27293534.

[23] Kim TK. Understanding one-way ANOVA using conceptual figures. Korean J Anesthesiol 2017;70(1):22–26. doi:10.4097/kjae.2017.70.1.22, PMID:28184262.

[24] Jada SR, Hamzah AS, Lajis NH, Saad MS, Stevens MF, Stanslas J. Semisynthesis and cytotoxic activities of andrographolide analogues. J Enzyme Inhib Med Chem 2006;21(2):145–155. doi:10.1080/14756360500499988, PMID:16789428.

[25] Jiang X, Yu P, Jiang J, Zhang Z, Wang Z, Yang Z, *et al*. Synthesis and evaluation of antibacterial activities of andrographolide analogues. Eur J Med Chem 2009;44(7):2936–2943. doi:10.1016/j.ejmech.2008.12.014, PMID:19152987.

[26] Genheden S, Ryde U. The MM/PBSA and MM/GBSA methods to estimate ligand-binding affinities. Expert Opin Drug Discov 2015;10(5):449–461. doi:10.1517/17460441.2015.1032936, PMID:25835573.

[27] Hayes JM, Archontis G. MM-GB(PB)SA Calculations of Protein-Ligand Binding Free Energies. In: Wang L (ed). Molecular Dynamics - Studies of Synthetic and Biological Macromolecules. London: IntechOpen; 2012. doi:10.5772/37107.

[28] Katsila T, Spyroulias GA, Patrinos GP, Matsoukas MT. Computational approaches in target identification and drug discovery. Comput Struct Biotechnol J 2016;14:177–184. doi:10.1016/j.csbj.2016.04.004, PMID:27293534.

[29] Lipinski CA, Lombardo F, Dominy BW, Feeney PJ. Experimental and computational approaches to estimate solubility and permeability in drug discovery and development settings. Adv Drug Deliv Rev 2001;46(1-3):3–26. doi:10.1016/s0169-409x(00)00129-0, PMID:11259830.

[30] Lee MS, Olson MA. Comparison of volume and surface area nonpolar sol- vation free energy terms for implicit solvent simulations. J Chem Phys 2018;139(4):044119. doi:10.1063/1.4819023.

[31] Wu R, Lu Z, Cao Z, Zhang Y. Zinc chelation with hydroxamate in histone deacetylases modulated by water access to the linker binding channel. J Am Chem Soc 2011;133(16):6110–6113. doi:10.1021/ja111104p, PMID:21456530.

[32] Zhang H, Li S, Si Y, Xu H. Andrographolide and its derivatives: Current achievements and future perspectives. Eur J Med Chem 2021;224:113710. doi:10.1016/j.ejmech.2021.113710, PMID:34315039.

[33] Wong CC, Lim SH, Sagineedu SR, Lajis NH, Stanslas J. SRJ09, a promising anticancer drug lead: Elucidation of mechanisms of antiproliferative and apoptogenic effects and assessment of in vivo antitumor efficacy. Pharmacol Res 2016;107:66–78. doi:10.1016/j.phrs.2016.02.024, PMID:26940565.

[34] Jada SR, Matthews C, Saad MS, Hamzah AS, Lajis NH, Stevens MF, *et al*. Benzylidene derivatives of andrographolide inhibit growth of breast and colon cancer cells in vitro by inducing G(1) arrest and apoptosis. Br J Pharmacol 2008;155(5):641–654. doi:10.1038/bjp.2008.368, PMID:18806812.